

University of Texas Rio Grande Valley

ScholarWorks @ UTRGV

---

Mechanical Engineering Faculty Publications  
and Presentations

College of Engineering and Computer Science

---

8-13-2012

## Adding Autonomic Healing Capabilities to Polyethylene Oxide

Dorina M. Chipara

*The University of Texas Rio Grande Valley*, dorina.chipara@utrgv.edu

Maritza Flores

*The University of Texas Rio Grande Valley*

Alma Perez

*The University of Texas Rio Grande Valley*

Nancy Puente

*The University of Texas Rio Grande Valley*

Karen Lozano

*The University of Texas Rio Grande Valley*, karen.lozano@utrgv.edu

*See next page for additional authors*

Follow this and additional works at: [https://scholarworks.utrgv.edu/me\\_fac](https://scholarworks.utrgv.edu/me_fac)

 Part of the [Mechanical Engineering Commons](#)

---

### Recommended Citation

Chipara, D.M., Flores, M., Perez, A., Puente, N., Lozano, K. and Chipara, M. (2013), Adding Autonomic Healing Capabilities to Polyethylene Oxide. *Adv. Polym. Technol.*, 32: E505-E513. doi:10.1002/adv.21296

This Article is brought to you for free and open access by the College of Engineering and Computer Science at ScholarWorks @ UTRGV. It has been accepted for inclusion in Mechanical Engineering Faculty Publications and Presentations by an authorized administrator of ScholarWorks @ UTRGV. For more information, please contact [justin.white@utrgv.edu](mailto:justin.white@utrgv.edu), [william.flores01@utrgv.edu](mailto:william.flores01@utrgv.edu).

---

**Authors**

Dorina M. Chipara, Maritza Flores, Alma Perez, Nancy Puente, Karen Lozano, and Mircea Chipara

---



# Adding Autonomic Healing Capabilities to Polyethylene Oxide

---

**DORINA MAGDALENA CHIPARA**

*Department of Physics and Geology, The University of Texas–Pan American, Edinburg, TX 78539*

**MARITZA FLORES**

*Department of Chemistry, The University of Texas–Pan American, Edinburg, TX 78539*

**ALMA PEREZ, NANCY PUENTE, KAREN LOZANO**

*Department of Mechanical Engineering, The University of Texas–Pan American, Edinburg, TX 78539*

**MIRCEA CHIPARA**

*Department of Physics and Geology, The University of Texas–Pan American, Edinburg, TX 78539*

Received: December 29, 2011

Accepted: June 15, 2012

**ABSTRACT:** The addition of autonomic healing (frequently defined as self-healing) capabilities to a water-soluble polymer (polyethylene oxide, PEO) is for the first time reported. The self-healing system consists of urea-formaldehyde microcapsules filled with dicyclopentadiene and first-generation Grubbs catalyst, dispersed within polyethylene oxide. Raman spectroscopy, optical microscopy, electron microscopy, and thermogravimetric analysis were used to characterize

Correspondence to: Mircea Chipara; e-mail: chipara@yahoo.com.

Contract grant sponsor: National Science Foundation under DMR.

Contract grant number: 0934157.

Contract grant sponsor: U.S. Army Research Laboratory.

Contract grant sponsor: U.S. Army Research Office.

Contract grant number: W911NF-08-1-0353.

this autonomic healing system. Self-healing capabilities were confirmed by mechanical testing (load–displacement, engineering stress–engineering strain, and true stress–true strain dependences) recorded at very slow elongation rates (0.01 mm/s). The testing fate was chosen to allow for the complete consumption of the monomer before fracture (the polymerization kinetics of PEO was estimated from Raman measurements). © 2012 Wiley Periodicals, Inc. *Adv Polym Techn* 32: E505–E513, 2013; View this article online at [wileyonlinelibrary.com](http://wileyonlinelibrary.com). DOI 10.1002/adv.21296

**KEY WORDS:** Mechanical properties, Microscopy, Raman spectroscopy, Self-healing, Thermogravimetric analysis (TGA)

## Introduction

Polymeric materials (PM) subjected to external stresses are failing if the external stress exceeds a certain threshold value. This feature affects the performance of PM, restricting their use in certain applications such as structural materials. An elegant technique to ameliorate the behavior of PM subjected to stresses has been recently proposed<sup>1–7</sup> and named as an autonomic healing process or simply either autonomic healing or self-healing. Frequently, this process is known as polymer self-healing. The technique, initially designed for low-molecular mass polymers or resins,<sup>7</sup> was later extended to high-molecular mass polymers<sup>8,9</sup> and to polymer-based (nano)composites.<sup>4,9</sup> The addition of self-healing capabilities involves the dispersion of some microcapsules filled with monomer and of catalysts within the liquid resin, homogenization of this complex mixture, and finally the polymerization of the resin. Typically, the monomer of choice is dicyclopentadiene (DCPD) and the associated catalyst is the first-generation Grubbs catalyst (FGGC). The encapsulation of DCPD within urea-formaldehyde is described elsewhere.<sup>10–12</sup> Under the effect of external stresses, the microcapsule filled with a monomer is eventually ruptured and its content is spilled out within the (epoxy) resin.<sup>1–9</sup> The released molecules of monomer will diffuse within the (epoxy) resin until they will encounter a catalyst particle, when (and where) a ring-opening polymerization will be ignited between the monomer (DCPD) that was confined within the microcapsule and the catalyst (FGGC). This finally results in the growth of a new macromolecular chain within the growing cracks of the polymer subjected to mechanical stresses. The self-healing has been confirmed by spectroscopic

techniques (mostly Raman spectroscopy<sup>13,14</sup>), which demonstrated the consumption of the monomer and the formation of the polymer, polydicyclopentadiene (PDCPD)), by indirect thermal methods,<sup>14</sup> and by mechanical testing (such as crack propagation,<sup>5,6</sup> stress–strain measurements,<sup>8</sup> and fatigue tests<sup>15</sup>). The limits and the weaknesses of the autonomic self-healing process based on urea-formaldehyde microcapsules filled with DCPD have been critically reviewed.<sup>16,17</sup> Few years ago, a new path to add self-healing polymers to polymers was described.<sup>8</sup> The authors dissolved the polymeric matrix in a solvent that does not affect the microcapsules and does not deactivate the Grubbs catalyst.<sup>5</sup> The same novel path is exploited now to add self-healing capabilities to polyethylene oxide (PEO)—a water-soluble polymer. The paper describes for the first time the addition of self-healing capabilities to a water-soluble polymer—an effort that may open a door toward biological and biomedical applications of self-healing (bio)polymers. The investigated samples contained 10(wt% microcapsules filled with DCPD (both PEO-REF and PEO-SH) and the PEO-SH series contained 0.5 wt% FGGC.

## Experimental

The following chemicals were purchased to add self-healing capabilities to PEO: PEO, characterized by an average molecular weight of 100,000 from Alfa-Aesar (Ward Hill, MA), DCPD research grade from Sigma-Aldrich (St. Louis, MO), FGGC from Sigma-Aldrich, and deionized water. The microcapsules were synthesized as reported elsewhere.<sup>10,11,18,19</sup> The list of chemicals (including quantities, details about vendors,

and description of the synthesis process) used to obtain polyurea formaldehyde (PUF) microcapsules are given elsewhere.<sup>10–19</sup> Autonomic healing capabilities have been added to PEO by using the following solution path: PEO (10 g) was dissolved in deionized water (300 mL). Powder of FGGC was added to the PEO solution and mixed for 30 min at 500 rotations per minute (rpm). An amount of 2 g microcapsules filled with DCPD was added, and the resulting system was gently mixed (below 250 rpm) for 30 min, poured onto glass slides covered with aluminum foil, and left to dry to evaporate the water content. We did notice that the nature of the substrate affects significantly the morphology of PEO and its mechanical features. These samples of PEO with self-healing capabilities were labeled PEO-SH. Such samples contain the polymer (PEO), the microcapsules filled with DCPD, and the Grubbs catalyst. Reference PEO samples were also obtained by dispersing the polymer in water and adding the same amount of microcapsules filled with DCPD (from the same batch, i.e., with the same size distribution). These samples were labeled PEO-REF and did not have autonomic healing capabilities due to the absence of the Grubbs catalyst. Nevertheless, a weak relaxation of the mechanical stresses and enhancement of mechanical properties may be due to the release of the monomer, which eventually will lubricate the slippage of macromolecular chains, each relative to other, at the beginning of the mechanical testing. The solvent-induced self-healing of polymers<sup>20</sup> exploits this feature. After a gentle mixing of components, each sample (PEO-SH and PEO-REF) was poured onto glass slides covered with aluminum foil and left to dry to evaporate the water content. Finally, the PEO-SH and PEO-REF films were peeled from the aluminum foils.

Optical microscopy data were obtained by using a Nikon Olympus BX51 microscope (Nikon Instruments Inc., Melville, NY). A field emission scanning electron microscope (SEM), model Sigma VP from Zeiss (Carl Zeiss NTS, LLC, Peabody, MA), was utilized to obtain the micrographs of microcapsules. Samples were glued to an SEM aluminum mount using double-sided adhesive tabs (Electron Microscopy Sciences, Hatfield, PA) and coated by sputtering with a thin metallic layer (to avoid electrical charging of nonconductive specimens). The sputtering was done by using a model Desk II system (Denton Vacuum, LLC, Moorestown, NJ) equipped with a gold-palladium target. Sputtering current was 40 mA, sputtering time 30 s, and chamber vac-

uum below 50 MTorr for a deposition rate of about 100 Å/min.

Raman spectroscopy measurements were performed on microcapsules, pristine PEO, PEO-REF, and PEO-SH samples, by using a Bruker Senterra (Bruker Optics, Billerica, MA) microRaman (confocal) instrument equipped with a laser diode operating at 785 nm (to reduce the fluorescence). The polymerization of DCPD in the presence of a FGGC was monitored by Raman spectroscopy. The in situ polymerization of DCPD in block copolymers loaded with microcapsules filled with DCPD and FGGC after the application of a mechanical stress was reported earlier.<sup>8</sup> In a mixture of DCPD–FGGC, containing 5% Grubbs catalyst, the monomer was almost completely used in about 1 h. In block copolymers loaded with microcapsules filled with DCPD and Grubbs catalyst, the monomer was exhausted in about 100 min.<sup>8</sup> This suggests that the time of the order of 2 h is sufficient not only to ignite the self-healing process but also to exhaust the monomer available to polymerization. Same timescales for ring-opening polymerization mediated by FGGC have been reported elsewhere.<sup>21,22</sup> To avoid the overheating of the sample, the power of the incoming laser beam was kept at 10 mW. Accordingly, the number of accumulations was increased resulting in a total time for the recording of the whole Raman spectrum of about 15–30 min depending on the spectral range. Thermogravimetry analysis (TGA) was performed on PUF microcapsules by using a TA Instruments (TGA Q500) equipment, operating in nitrogen atmosphere, at a heating rate of 10°C/min. Mechanical tests were performed by using a TestResources (1000 R44 mechanical tester; Shakopee, MN) equipment operating according to ASTM D 1708 “Standard Test Method for Tensile Properties of Plastics by Use of Microtensile Specimens.” Sets consisting of at least six samples of dog bone shape (for each PEO-SH and PEO-REF series) were tested and statistically analyzed.

## Results and Discussion

PUF microcapsules filled with DCPD were obtained by polymerization in emulsion, as reported elsewhere.<sup>10–19</sup> The stirring rate for this synthesis was 400 rpm, the pH was kept at 3.5, and the reaction temperature was set at 55°C. The synthesis of microcapsules was stopped after 5 h.

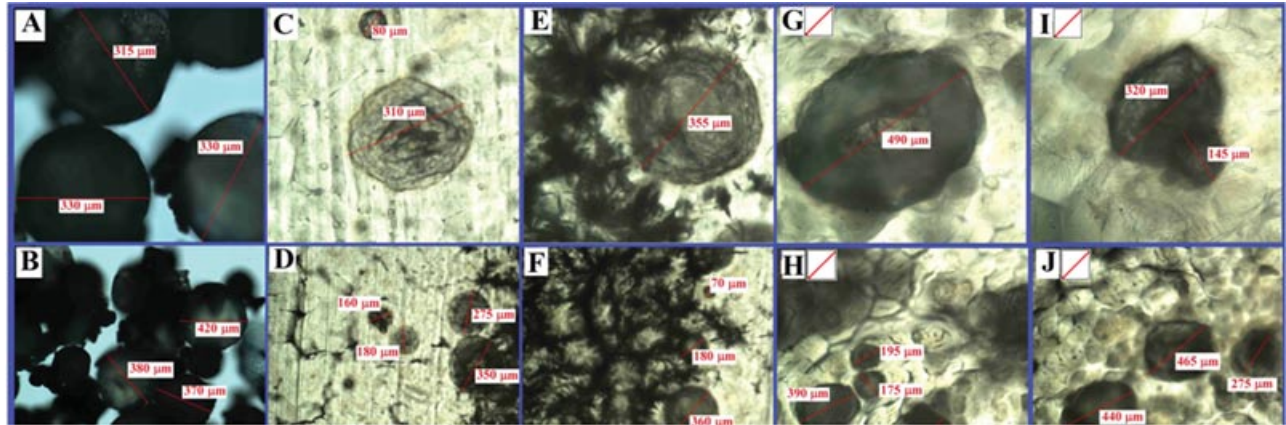


**FIGURE 1.** Optical microscopy photographs of the as obtained microcapsules filled with DCPD (1A and 1B). Photos of microcapsules dispersed within PEO-REF samples (1C to 1F). Optical microscopy photographs of PEO-REF samples subjected to mechanical stresses (1G–1J). The arrow included in the left upper corner defines the direction of the applied force.

Optical microscopy photographs of the as obtained microcapsules filled with DCPD revealed a relatively narrow distribution of microcapsules' diameters with an average of about 360 μm (see Figs. 1A and 1B). The microcapsules dispersed within PEO (PEO-REF samples) are shown in Figs. 1C–1F. A slight drop in the diameter of the

microcapsules is noticed and assigned eventually to the pressure exerted by the polymeric matrix on microcapsules. Figures 1G–1J show the optical microscopy photographs of the PEO-REF samples subjected to mechanical stress. The arrow included in the left upper corner defines the direction of the applied force. The distortion of the microcapsules

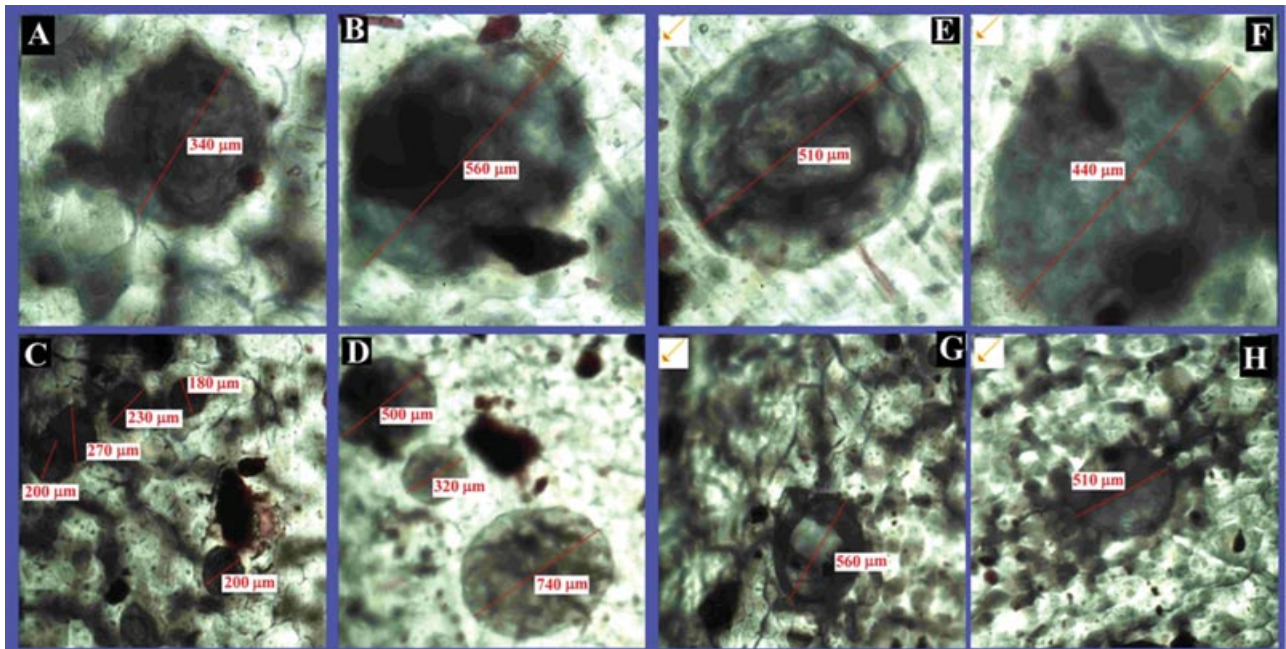


**FIGURE 2.** The optical microscopy photographs for the series PEO-SH. Photos of microcapsules and FGFC dispersed within PEO (2A–2D). FGFC is easily recognized by its dark red color. Photos of mechanically stretched PEO-SH samples (2E–2H). As in the previous case, the microcapsules are elongated along the direction of the external stress (see the arrow in the inset of Fig. 2E–2H).

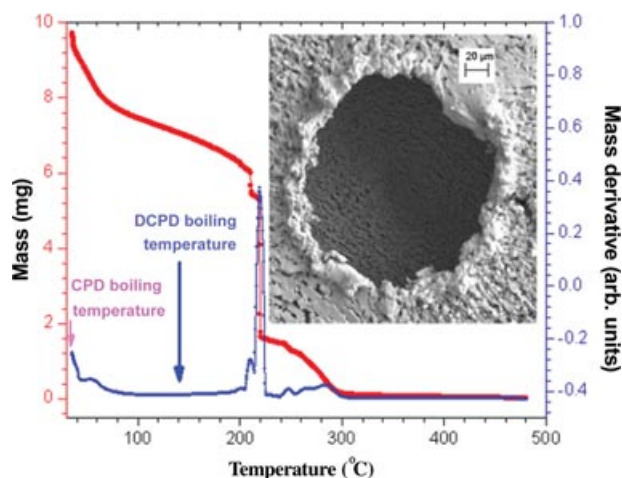


**FIGURE 3.** TGA thermograms of PUF microcapsules filled with DCPD performed in nitrogen. SEM photograph of a microcapsule is shown in the inset.

along the direction of the applied force is observed. The same kind of distortion of the shape of microcapsule was reported in self-healed block copolymers.<sup>8</sup>

The optical microscopy photographs for the series PEO-SH are shown in Fig. 2. The first group of photographs (Figs. 2A–2D) shows both the microcapsules and the FGFC dispersed within the polymer. FGFC is easily recognized by its dark red color. It is noticed that the catalyst particles have a broad size distribution with chunks of the order of 100  $\mu\text{m}$ . This indicates that the stirring is not an efficient procedure for the dispersion of the Grubbs catalyst. The second group of photographs (Figs. 2E–2H) shows the mechanically stretched PEO-SH samples. As in the preceding case, the microcapsules are elongated along the direction of the external stress (see the arrow in the inset of Figs. 2E–2H).

TGA tests were performed in nitrogen atmosphere to estimate the amount of DCPD within the PUF microcapsules (see Fig. 3). The measurements were performed 1 day after the synthesis of microcapsules filled with DCPD and after 2 months after the synthesis of microcapsules (stored in air at room temperature). TGA data revealed a residual amount of DCPD of about 55% after a 2-month storage. This suggests that the wall of the microcapsule is thick, and consequently more stress is required to achieve the rupture of the microcapsules. As reported elsewhere,<sup>3–6</sup> this reflects an excess of formaldehyde and drops the self-healing efficiency. Nevertheless, the amount of DCPD within the microcapsules dispersed in the PEO matrix is higher, due to relatively low diffusion coefficient

of the monomer through PEO. SEM measurements (shown as an inset of Fig. 3) confirmed that PUF microcapsules have a thick wall (of the order of micrometers). The rapid drop in the mass of microcapsules at about 210°C corresponds to the thermal degradation of the wall of the microcapsules through volatilization of the labile units.

Raman spectroscopy is a powerful tool in the investigation of PM and in particular in the study of self-healing polymers.<sup>13,22,23</sup> PEO exhibits a complex Raman spectrum. At fairly low Raman shifts (typically below 50  $\text{cm}^{-1}$ ), PEO exhibits with strong lines assigned to the longitudinal acoustic mode—LAM (this part of the Raman spectrum is not accessible to our spectrometer<sup>24</sup>). For Raman shifts ranging between 200 and 400  $\text{cm}^{-1}$ , Raman lines assigned to the so-called D-LAM have been reported elsewhere.<sup>23</sup> Typically, the Raman lines of PEO are affected by the chain conformation,<sup>23</sup> water content, and crystallinity. Figure 4 shows the actual Raman spectra of PEO-SH and PEO-REF, which includes assignments of most important peaks (for PEO, DCPD,<sup>25</sup> and DCPD polymerization<sup>14</sup>). Raman spectroscopy of the series of PEO-REF subjected to mechanical stresses confirmed the presence of DCPD within microcapsules (see Fig. 4) and showed that the amount of residual DCPD is less (almost negligible) near the fractured microcapsule, confirming the stress-induced release of DCPD. Similar Raman spectra were obtained for the PEO-SH series before and immediately (about 30 min) after fracture. As expected, the presence of catalysts resulted in the disappearance of the DCPD peak in stretched PEO-SH samples and the observation of the Raman spectrum due to PDCPD.<sup>13,14,22</sup>

Figure 5 shows a relevant region of the Raman spectrum for PEO loaded with microcapsules filled with DCPD, and for the PEO-SH sample, before and after stretching. The typical Raman lines of DCPD located at 1570 and 1615  $\text{cm}^{-1}$  and assigned to DCPD are almost completely disappeared in about 2 h because the (fast) stretching of the sample.<sup>2,13</sup> A weak and broad signal assigned to PDCPD is noticed at about 1670  $\text{cm}^{-1}$ . The same broad line was reported in self-healed block copolymers.<sup>8</sup> To confirm the self-healing capabilities, mechanical tests on six identical series of samples PEO-REF and PEO-SH were performed. To sense the self-healing capabilities, load-displacement dependencies at very low extension rates (0.01 mm/s) were performed. The slow speed of the mechanical test allowed for the rupture of microcapsules, monomer release, and ignition of polymerization reactions. According to Raman data, all

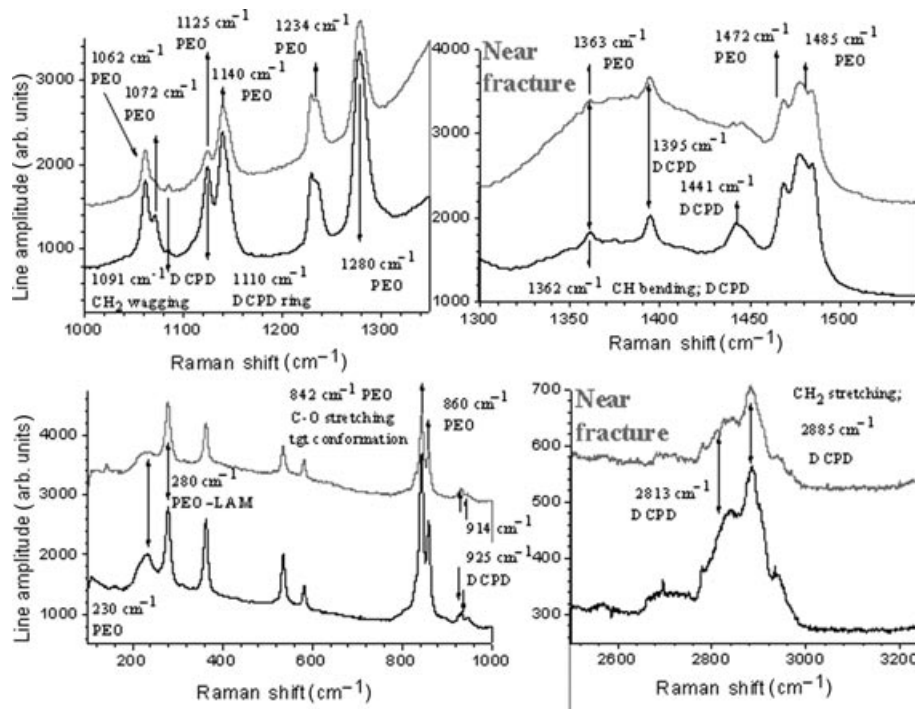


**FIGURE 4.** Raman spectra of PEO-REF and PEO-SH samples before and after stretching.

monomer is exhausted before the fracture of the sample (typically, the time required to achieve the mechanical testing ranged between 2 and 3 h). The as-obtained data were statistically analyzed for two ensembles (PEO-REF and PEO-SH), each containing at least six samples prepared in identical conditions. Mechanical testing confirmed the activation of self-healing capabilities in the series PEO-SH. Figure 6 shows a typical load–displacement dependence for a pair PEO-SH and PEO-REF. The top panel of Fig. 7 shows the dependence of engineering stress versus the engineering strain, and the bottom panel of Fig. 7 depicts the dependence of the true stress versus true strain. The engineering stress was calculated as the ratio between the applied load and the initial surface of the sample, whereas the true strain included the correction due to the change in the cross section of the sample during the uniaxial extension. The statistical analysis of the mechanical properties of PEO-SH and PEO-REF revealed a large dispersion of experimental data (elongation at break and tensile strength), mainly for the PEO-SH series. This suggests that an important cause of the broad dispersion of experimental data in PEO-SH series originates from the nonuniform size and distribution of the catalyst. The statistical analysis

showed that the average value of the elongation at break for PEO-SH is equal to 92 mm and for PEO-REF only 66 mm but the standard deviation is 20 mm for PEO-REF and 30 mm for PEO-SH. Similarly, the ultimate load is about  $2.51 \pm 0.01$  N for PEO-REF and  $3.35 \pm 0.01$  N for PEO-SH with the standard deviation of 0.50 N for PEO-REF and 0.60 N for PEO-SH. Most importantly, Fig. 7 shows eloquently that the self-healing features are present even when using the engineering and the true stresses and strains.

These results confirmed the addition of self-healing capabilities to PEO. However, they can be further improved by

1. A partial deactivation of the FGCC or a drop in the polymerization reaction is possible. Our preliminary Raman studies revealed no qualitative change in the kinetics of the monomer consumption compared to the system polystyrene–polybutadiene–polystyrene. Nevertheless, our errors in the analysis of the monomer consumption rate are rather large, as the time to record a full Raman spectrum was up to 30 min. Additional studies to assess the kinetics of DCPD polymerization in PEO are

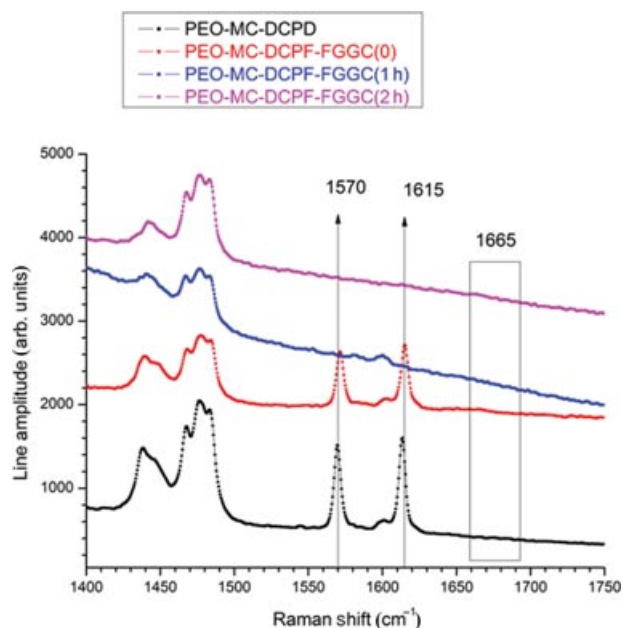


**FIGURE 5.** Raman spectra of PEO-SH samples before and after stretching (0 hour, 1 hour and 2 hour), showing the ring-opening polymerization of DCPD.

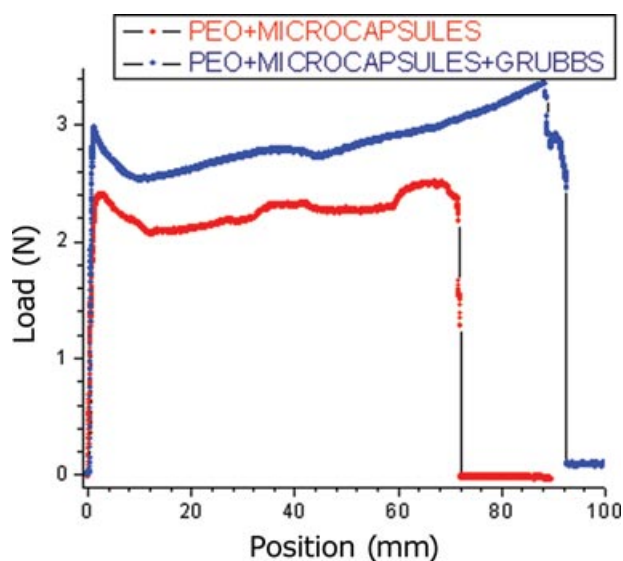


**FIGURE 6.** Typical load–displacement dependence for PEO-REF and PEO-SH showing the self-healing of PEO.

in course. While water has an adverse effect on the FGGC, it is important to mention that the self-healing process does not occur in water (the water has been removed from all PEO-REF and PEO-SH specimens by slow evaporation before mechanical stretching). TGA data

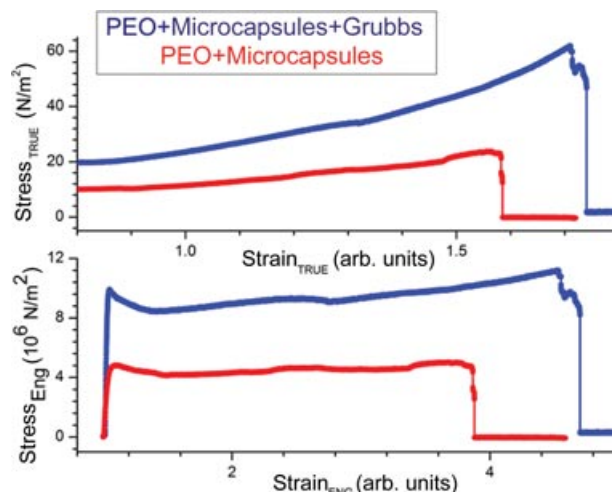


**FIGURE 7.** Dependence of (top) engineering stress on the engineering strain and (bottom) true stress versus true strain for PEO-REF and PEO-SH showing the self-healing of PEO.

confirmed water removal within an accuracy better than 1%.

2. The microcapsules that we used have a rather thick (about 1- $\mu\text{m}$ ) wall, and consequently some microcapsules may survive the sample's stretching.
3. Diminishing of the leakage of the monomer through the wall of microcapsules. This can eventually result in the polymerization of the monomer within the PEO matrix loaded with Grubbs catalyst before the application of the external load (which is the trigger for the self-healing process).<sup>26–28</sup>
4. The actual formulation (the concentration of DCPD and FGGC) has not been optimized. This may be an important factor as the diffusion coefficient of the DCPD within PEO can be lower than in our previous system.
5. The method used to assess the self-healing capabilities (slow strain–stress experiments) implies a complex behavior of the specimen. In the first 30 min, there is not significant consumption of the monomer and consequently the stress–strain dependence is dominated by the non–self-healing behavior. During the next 60 min, the monomer is released and a lubrication of macromolecular chain relative motion becomes possible. This solvent-induced self-healing<sup>20</sup> can explain the increase in the elongation or strain in the self-healing

specimen compared to the reference ones. After 2 h, Raman data suggest that all monomer was exhausted. However, the polymer grown inside the cracks is eventually a high-viscosity oligomer. This contributes to the increase of the ultimate load/stress.

While the results support the addition of self-healing features, further effort is required to determine the optimum concentrations of the components and to decrease the dispersion of experimental data. The decrease in the wall of the microcapsule is another important parameter that has to be controlled to enhance the self-healing of PEO. A particular attention has to be paid to the size distribution of the Grubbs catalyst, perceived as an important factor in the broadening of experimental data.

## Conclusions

Self-healing capabilities were successfully added—for the first time—to a water-soluble polymer (PEO). This opens a door toward biological and biomedical applications of self-healing polymers and justifies future research. It was noticed that the FGGC is not deactivated by water. Optical and scanning electron microscopy techniques were used to assess the size (diameter) of the microcapsules and the thickness of the microcapsule's wall. Scanning electron microscopy revealed a thick wall, probably due to the amount of urea-formaldehyde and long reaction time.

Self-healing capabilities were tested by stress-strain measurements at very low strain rates. The statistical analysis of experimental data revealed an enhanced mechanical strength of the self-healed samples compared to the reference ones. However, the dispersion of experimental data was broad, probably due to a wide distribution of the size of the Grubbs catalyst. While the tests confirmed the self-healing, the enhancement of mechanical properties was not remarkable, being typically weaker than in the case of styrene-isoprene block copolymers. Nevertheless, it is possible to further enhance the benefits of the self-healing approach by searching for the optimum concentration of microcapsules and FGGC, for the best thickness of the microcapsule wall's thickness, and for the best size of microcap-

sules. In the research reported here, the formulation of the self-healing system was similar to the one used for rubbery block copolymers. There is a significant difference in the value of the diffusion coefficient in materials above and below the glass transition temperature, which can justify the need for a different composition of the self-healing system.

## References

1. Wool, R. P. *Nature* 2001, 409, 773–774.
2. White, S. R.; Sottos, N. R.; Geubelle, P. H.; Moore, J. S.; Kessler, M. R.; Sriram, S. R.; Brown, E. N.; Viswanathan, S. *Nature* 2001, 409(6822), 794–797.
3. Brown, E. N.; Kessler, M. R.; Sottos, N. R.; White, S. R. *J Microencapsulation* 2003, 20(6), 719–730.
4. Kessler, M.; Sottos, N.; White, S. *Composites, Part A* 2003, 34(8), 743–753.
5. Brown, E.; Sottos, N. R.; White, S. R. *Exp Mech* 2002, 42(4), 372–379.
6. Kessler, M.; White, S. *Composites, Part A* 2001, 32(5), 683–699.
7. Wilson, G. O.; Moore, J. S.; White, S. R.; Sottos, N. R.; Anderson, H. M. *Adv Funct Mater* 2008, 18(1), 44–52.
8. Chipara, M. D.; Chipara, M.; Shansky, E.; Zaleski, J. M. *Polym Adv Technol* 2009, 20(4), 427–431.
9. Mauldin, T. C.; Kessler, M. R. *Int Mater Rev* 2010, 55(6), 317–346.
10. Brown, E. N.; Kessler, M. R.; Sottos, N. R.; White, S. R. *J Microencapsulation* 2003, 20(6), 719–30.
11. Ting, Z.; Min, Z.; T. Xiao-Mei, Z.; Feng, C. *J Appl Polym Sci* 2010, 115, 2162–2169.
12. Yuan, L.; Gu, A.; Liang, G. *Mater Chem Phys* 2008, 110(2–3), 417–425.
13. Ding, F.; Monsaert, S.; Drozdak, R.; Dragutan, I.; Dragutan, V.; Sun, Y.; Gao, E.; Van Der Voort, P.; Verpoort, F. *Vib Spectrosc* 2009 51(2), 147–151.
14. Barnes, S. E.; Brown, E. C.; Corrigan, N.; Coates, P. D.; Harkin-Jones, E.; Edwards, H. G. M. *Spectrochim Acta, Part A* 2005, 61(13–14), 2946–2952.
15. Keller, M. W.; White, S. R.; Sottos, N. R. *Polymer* 2008, 49(13–14), 3136–3145.
16. Chipara, M.; Wooley, K. *Mater Res Symp Proc* 2005, 851, NN4.3.1.
17. Wu, D. Y.; Meure, S.; Solomon, D. *Prog Polym Sci* 2008, 33(5), 479–522.
18. Fan, C.; Zhou, X. *Colloids and Surfaces, A* 2010, 363(1–3), 49–55.
19. Hong, K.; Park, S. *J Mater Sci* 1999, 34, 3161–3164.
20. Caruso, M. M.; Delafuente, D. A.; Ho, V.; Sottos, N. R.; Moore, J. S.; White, S. R. *Macromolecules* 2007, 40(25), 8830–8832.

## ADDING AUTONOMIC HEALING CAPABILITIES TO POLYETHYLENE OXIDE

21. Ding, F.; Yu, B.; Monsaert, S.; Sun, Y.-G.; Gao, E.; Dragutan, I.; Dragutan V.; Verpoort, F. *Spectrochim Acta, Part A* 2010, 77, 170–174.
22. Schaubroeck, D.; Brughmans, S.; Vercaemst, C.; Schaubroeck, J.; Verpoort, F. *J Molec Catal A: Chem* 2006, 254(1–2), 180–185.
23. Todica, M.; Pop, C. V.; Dinte, E.; Farcau, C.; Astilean, S. *Mod Phys Lett B* 2007, 21(16), 987–995.
24. Kim, I. *Macromolecules* 1996, 29(9), 7186–7192.
25. Gallinella, E.; Fortunato, B.; Mirone, P. *J Molec Spectrosc* 1967, 24(1–4), 345–362.
26. Yuan, L.; Liang, G.-Z.; Xie, J.-Q.; Li, L.; Guo, J. *J Mater Sci* 2007, 42(12), 4390–4397.
27. Yuan, L.; Liang, G.; Xie, J.; Li, L.; Guo, J. *Polymer* 2006, 47(15), 5338–5349.
28. Li, B.; Dong, G.; Zhang, C. *J Appl Polym Sci* 2011, 122, 1450–1456.